Melting and dissociation of ammonia at high pressure and high temperature

J. G. O. Ojwang, R. Stewart McWilliams, Xuezhi Ke, and Alexander F. Goncharov

Citation: J. Chem. Phys. **137**, 064507 (2012); doi: 10.1063/1.4742340
View online: http://dx.doi.org/10.1063/1.4742340
View Table of Contents: http://jcp.aip.org/resource/1/JCPSA6/v137/i6
Published by the American Institute of Physics.

Additional information on J. Chem. Phys.

Journal Homepage: http://jcp.aip.org/
Journal Information: http://jcp.aip.org/about/about_the_journal
Top downloads: http://jcp.aip.org/features/most_downloaded
Information for Authors: http://jcp.aip.org/authors

ADVERTISEMENT

Melting and dissociation of ammonia at high pressure and high temperature

J. G. O. Ojwang,[1,2] R. Stewart McWilliams,[1,3] Xuezhi Ke,[4] and Alexander F. Goncharov[1,a)]
[1]*Geophysical Laboratory, Carnegie Institution of Washington, 5251 Broad Branch Rd. NW, Washington, DC 20015, USA*
[2]*Department of Radiation Oncology, Wake Forest University Health Sciences, Winston-Salem, North Carolina 27157, USA*
[3]*Howard University, Washington, DC 20059, USA*
[4]*Department of Physics, East China Normal University, Shanghai 200062, China*

(Received 25 March 2012; accepted 16 July 2012; published online 14 August 2012)

Raman spectroscopy and synchrotron x-ray diffraction measurements of ammonia (NH_3) in laser-heated diamond anvil cells, at pressures up to 60 GPa and temperatures up to 2500 K, reveal that the melting line exhibits a maximum near 37 GPa and intermolecular proton fluctuations substantially increase in the fluid with pressure. We find that NH_3 is chemically unstable at high pressures, partially dissociating into N_2 and H_2. *Ab initio* calculations performed in this work show that this process is thermodynamically driven. The chemical reactivity dramatically increases at high temperature (in the fluid phase at $T > 1700$ K) almost independent of pressure. Quenched from these high temperature conditions, NH_3 exhibits structural differences from known solid phases. We argue that chemical reactivity of NH_3 competes with the theoretically predicted dynamic dissociation and ionization. © *2012 American Institute of Physics*. [http://dx.doi.org/10.1063/1.4742340]

I. INTRODUCTION

The behavior of ammonia (NH_3) at high temperature and high pressure (HTHP) conditions is of fundamental scientific interest since it is expected to be one of the major constituents of the giant planets in our solar system.[1] Uranus and Neptune, for example, are thought to have "hot ice" layers (predominantly made up of 56% H_2O, 36% CH_4, and 8% NH_3 in solar proportions[2]) located between a rocky core and a gaseous atmosphere. Knowing the physical and chemical properties of NH_3 at HTHP (temperature $T > 2000$ K, pressure $P > 20$ GPa) is critical for understanding the observable properties (gravitational moments, atmospheric composition, and magnetic field) of these planets.[2–4]

It has been predicted that at HTHP, NH_3 becomes a protonic conductor in which the hydrogen atoms undergo rapid hops between neighboring molecules forming a superionic solid or ionic fluid.[2] Cavazzoni *et al.*,[2] using *ab initio* molecular dynamics (AIMD), predicted that above 60 GPa and 1200 K, NH_3 transforms from the $P2_12_12_1$ structure to a superionic solid with an hcp lattice of nitrogen atoms and highly mobile protons (Fig. 1, inset). At even more extreme conditions of pressure and temperature, molecules are expected to dissociate and react at very rapid rates.[2,5] Ionic properties are even predicted at low temperatures: Needs and Pickard,[6] using *ab initio* methods, suggested that above 90 GPa, the most stable phase of NH_3 is a disproportionated ionic solid (orthorhombic *Pma*2 structure) consisting of NH_2^- and NH_4^+ radicals.

Experiments using shock-wave compression have measured enhanced electrical conductivity in NH_3 at pressures near 40 GPa and 3000 K, consistent with ionization at these conditions,[3] yet direct chemical and structural data on this HTHP state have not been obtained. We used laser-heated diamond-anvil cells (DACs) combined with *in situ* Raman spectroscopy and x-ray diffraction (XRD) measurements of structure, melting, chemical speciation, and bonding to study the physical-chemical state of NH_3 to ~60 GPa, and ~2200 K (thereby extending HTHP studies of NH_3 in the DAC from ~10 GPa and ~1000 K (Refs. 7–13)). We report on novel chemical reactivity of NH_3 (Fig. 1) competing with previously outlined ionization phenomena.[2–5] In addition, the first-principles calculations performed in this work show that NH_3 chemically dissociates to N_2 and H_2 above approximately 7 GPa and 900 K driven by the entropy of mixing term in the free energy formulation.

II. EXPERIMENTAL METHODS

These studies were performed using symmetric DACs utilizing 300 μm anvil culets with tungsten or rhenium gasket materials. We used a gasket with a recessed hole with stepped diameters (inner diameter of 50–70 μm, outer diameter 100–120 μm) to form a sample cavity. The heat transfer to the sample was provided by an Ir (or compressed amorphous boron in control experiments) coupler of dimensions 90 × 90 × 10 μm, with 1–5 holes of 4–20 μm diameter, which rested on the recess in the gasket to isolate it from the anvils. Coupler holes formed sample chambers with minimized temperature gradients for *in situ* Raman/XRD measurements. The coupler was heated from both sides using a 1.075 μm Yb-based fiber laser. Temperature was measured using spectroradiometry, while pressure was determined by ruby fluorescence at room temperature. No thermal correction of pressure

a)Author to whom correspondence should be addressed. Electronic mail: agoncharov@ciw.edu.

 © 2012 American Institute of Physics

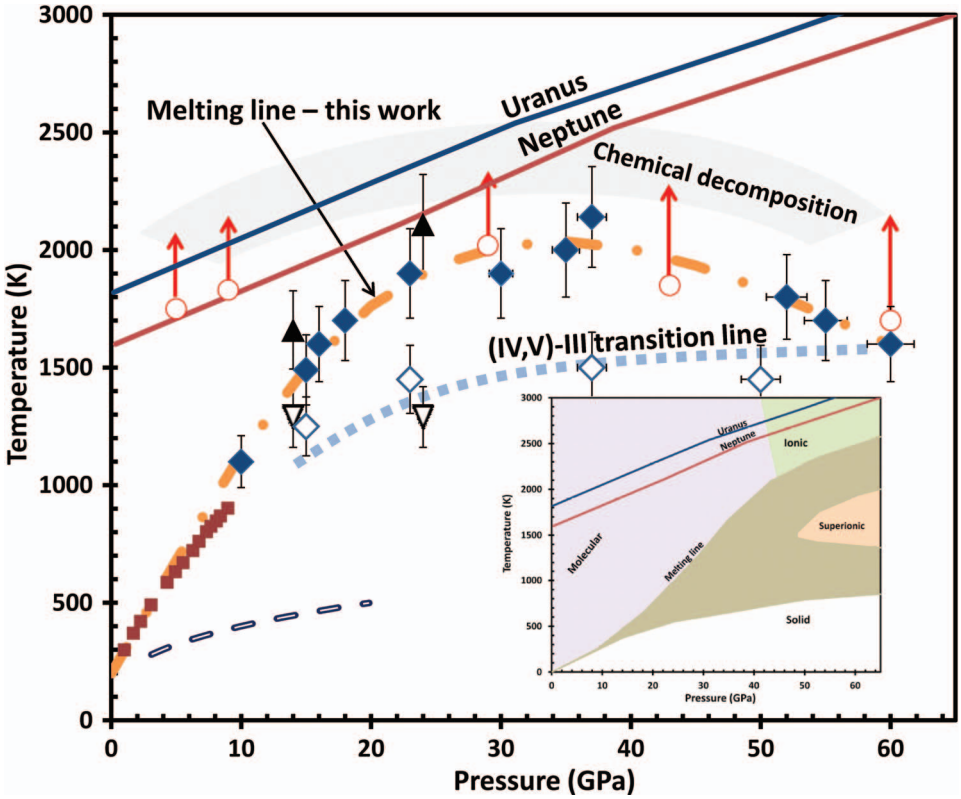

FIG. 1. Phase diagram of NH_3. The Uranus and Neptune isentropes are from Ref. 4. Filled triangles and diamonds represent synchrotron XRD and Raman measurements of the melting line in this study, respectively. The open triangles and diamonds indicate the observed solid-solid phase transitions in our synchrotron XRD and Raman studies, respectively (fitted with a dotted blue line). The open circles indicate the temperature prior to the appearance of flash. The chemical decomposition band, which is associated with flash, appearance of N_2 and H_2 in bulk quantities, and polymorphic modifications of NH_3 on quenching, is indicated by the gray region. The error bars in our measured T reflect the uncertainties (~200 K). The uncertainty in P is ~2 GPa. Our results for the melting line (the dashed-dotted orange line) are a fit of the Kechin melt equation:[35] $T_m(P) = T_0(1 + P/a)^b e^{-cP}$, where $a = 3.051$ GPa, $b = 1.466$, $c = 0.039$ GPa^{-1}, $T_0 = 200$ K, and P is in units of GPa. The solid squares and the open-rectangles dashed line show the previously reported melting points and the (IV,V)-III transition, respectively (Ref. 10). Inset: The phases proposed by Cavazzoni *et al.*[2] (solid, molecular, ionic, and superionic) are indicated by different colors.

(estimated to be <4 GPa at the highest temperature) was taken into consideration.

NH_3 was loaded into the DAC cryogenically as follows. The DAC was first cooled by immersion in liquid N_2 in a glove box purged with N_2 gas. When the cell achieved a temperature in the liquid range of NH_3, vapor of NH_3 was flushed into the DAC sample chamber using a hypodermic needle. Once the entire cell was fully flushed with NH_3, the needle was removed and the DAC was tightened, trapping the liquid NH_3 in the gasket. The DAC was then allowed to warm to room temperature after which it was pressurized to the desired pressure. For Raman studies, either the 457 nm or 488 nm lines from a solid state laser were used for excitation in the laser-heated DAC.[14] Infrared (IR) absorption measurements of the sample quenched to 300 K were performed using a Fourier transform spectrometer equipped with a custom made IR microscope and a liquid N_2 cooled mercury cadmium telluride detector. Synchrotron XRD data at HTHP were collected using a dedicated laser heating setup at the 13-ID beamline of GeoSoilEnviroCARS at the Advanced Photon Source.[15] The seats for the symmetric DAC were made from x-ray transparent cubic boron nitride (cBN) to ensure a large x-ray aperture, and permit measurements at $2\theta_{max} \leq 25^\circ$.

In our measurements (Figs. 2–4), XRD and Raman signals of solid and fluid phases coexist in a wide temperature range (up to 500 K based on the results of previous measurements and finite element calculations) due to axial temperature gradients, which is common for such measurements.[16,17] The transition temperatures were determined using the 50% intensity criterion. The results reported here are based on more than 20 sample loadings, which showed reproducible readings.

III. THEORETICAL METHODS

The first-principles total-energy calculations have been performed in the framework of density functional theory (DFT) (Refs. 18 and 19) using the local density approximation (Ceperley-Alder type) (Ref. 20) as implemented in the Vienna Ab initio Simulation Package (VASP) code.[21,22] The valence electron-core interaction was treated by the all-electron projector augmented wave method (PAW).[23,24] The k-point sampling was performed on a dense Monkhorst-Pack grid.[25] The electronic occupancies were determined from a Gaussian smearing algorithm with 0.1 eV smearing width, and the projection operators were evaluated in the reciprocal

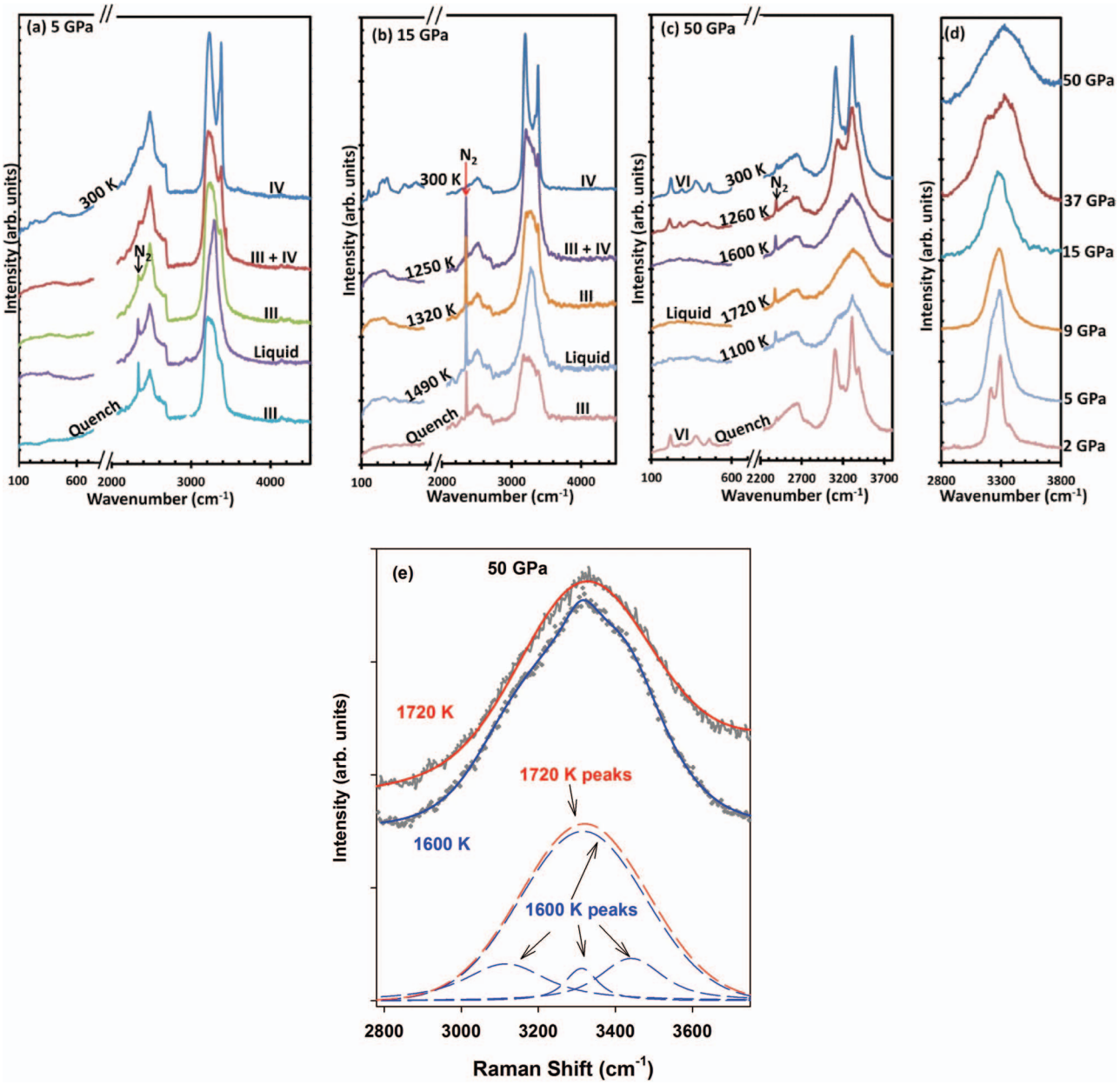

FIG. 2. Representative Raman spectral changes of NH_3 at (a) 5 GPa, (b) 15 GPa, and (c) 50 GPa as a function of temperature. The arrows indicate the N_2 vibrons. (d) Raman spectra of fluid phase at different pressures (the temperature was measured just above the melting line, see Fig. 1). In (a), temperatures were too low to measure with radiometry. The sample at 50 GPa is from a previous lower pressure heating run, which is why a weak N_2 vibron signal appears prior to the heating run shown in (c). In (e), we show the detailed vibron spectra through melting. The statistical data analysis shows that at 1600 K, the spectrum can be best fit by a superposition of narrow bands corresponding to solid and a broad band of fluid, while the spectrum at 1720 K can be equally well fit by a single broad band corresponding to fluid.

space. The energy cutoff for the plane wave expansion was set to 500 eV throughout the calculations. The configurations N $2s^2 2p^3$ and H $1s^1$ were treated as the valence electrons. The convergence of total energy with respect to the *k*-point mesh and energy cutoff was found to be less than 0.3 meV/atom. The unit cells at each volume were fully optimized until the Hellmann-Feynman forces were less than 0.001 eV/Å^2/atom. To obtain phonons, the direct *ab initio* force-constant approach was used, as implemented by Parlinski.[26,27] In this method, a specific atom is displaced to induce the forces to act on the surrounding atoms, which are calculated via the Hellmann-Feynman theorem. The magnitude of the displacement of 0.03 Å was used in our calculations. The forces were collected to form the force-constant matrices and then dynamical matrices. Harmonic phonons were obtained from the diagonalization of the dynamical matrices. Thermodynamic functions, including internal energy and Gibbs free energy, were evaluated from the integral of the phonon density of states.[28]

IV. RESULTS

Above 1.2 GPa, NH_3 crystallizes in an orientationally disordered cubic (*Fm*3*m*) phase (NH_3-III),[7,8] which transforms at 3.5 GPa and 300 K to NH_3-IV ($P2_12_12_1$ space group[9]). NH_3-IV and isostructural NH_3-V (stable above

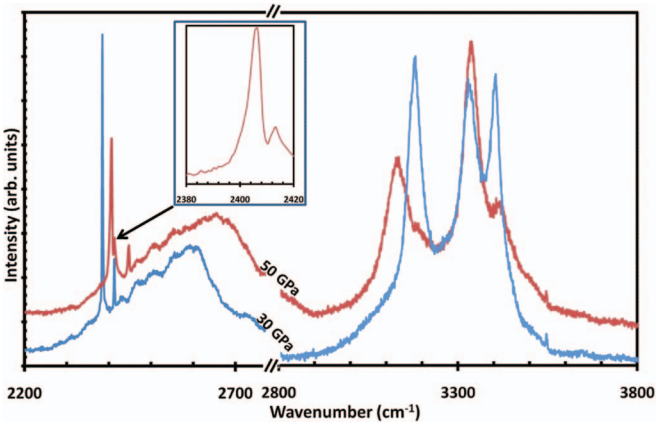

FIG. 3. Raman spectra of the products of laser-heated ammonia at different pressures. The Raman spectrum of nitrogen exhibits two major vibron bands characteristic of pure bulk N_2 (ν_1, ν_2). The inset shows a fine splitting of the ν_2 nitrogen vibron. The NH_3 sample at 30 GPa was heated until the appearance of N_2 (blue curve). When this sample was cold-compressed to 50 GPa (red curve), the lower-frequency (ν_2) peak, which is related to the N_2 molecules centered on the 6*c(D2d)* site, split into two peaks (inset). This splitting is associated with the distortion of the *Pm3n* (or formation of a low-symmetry) structure of pure N_2.[31]

15 GPa (Refs. 10 and 11)) are ordered phases with pronounced Raman-active lattice modes and are characterized by three Raman peaks in the N–H stretching region (Fig. 2(a)) with a weak central peak.[10] This spectral range contains ν_1 and ν_3 symmetric and asymmetric stretching fundamentals and also the overtones of the ν_4 bending mode coupled to ν_1. The phase transformation to NH_3-VI above 40 GPa (Refs. 12 and 13) is characterized by changes in the lattice mode region and also relative intensity change between the different components of the N–H stretch band (Fig. 2).

Raman data at elevated temperatures collected for different pressures (Fig. 2) show pronounced changes in the lattice and N–H stretch spectral regions signifying phase and bonding changes. As temperature increases, the lattice modes decrease in intensity concomitantly with the broadening of the N–H stretch modes (Fig. 2); we relate these changes to transformation to disordered NH_3-III. At higher temperatures, all N–H stretch bands merge into a single broad peak (Fig. 2), indicative of melting. These transformations in the bulk of NH_3 revealed by Raman spectroscopy are reversible (e.g., Fig. 2(c)) even in the presence of a moderate chemical reactivity (see below). These results are further confirmed in XRD (also see below). An N_2 vibron ($\sim$2350 cm^{-1}) appears at temperatures approaching that of the melt line implying that NH_3 partly decomposes into N_2 and H_2 in the solid phase (Fig. 2). A H_2 vibron was also observed in some experiments, but was more difficult to detect because hydrogen tends to diffuse from the probed area. The spectral positions and the number of N_2 and H_2 vibron lines correspond to that for solid phases of H_2 and N_2 in the studied pressure range (e.g., Refs. 29 and 30), which along with the lack of H_2 detection in the laser heated spot indicates that H_2 and N_2 phase separate from ammonia following dissociation (Fig. 3). In a regime of very intense chemical transformation attained at temperatures above the melt line (Fig. 4), we observed the irreversible formation of other polymorphic phases of NH_3 as will be discussed below.

Synchrotron XRD was used to verify the Raman spectroscopy observations concerning phase changes and melting (Fig. 5). XRD pattern changes observed under initial heating at 24 GPa (Fig. 5(a)) can be clearly identified with the IV(V)-III transition. At higher temperatures, we can see a substantial decrease in intensity of the Bragg peaks related to solid NH_3 and a broad diffuse scattering becomes visible (Fig. 5(b)); these observations are consistent with the melting of a large volume of sample.

Combining the results of Raman and XRD studies, the experimental phase lines are plotted in Fig. 1. The melting curve determined in our Raman and XRD experiments agrees

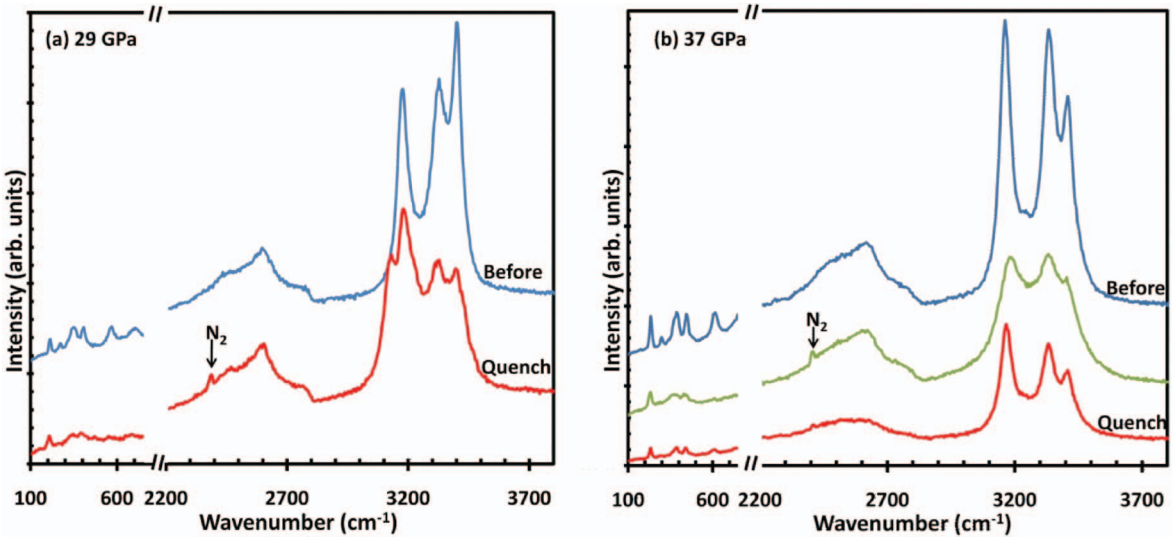

FIG. 4. Raman spectra illustrating reversible and irreversible phenomena in laser-heated ammonia-V. In (a), the sample was heated until the flash appeared. On quenching it is found that there is a split in the N–H band. In (b), the sample was heated until N_2 formed (middle trace) but without the appearance of the flash. The NH_3 Raman spectra before and after heating are similar. These experiments are reproducible.

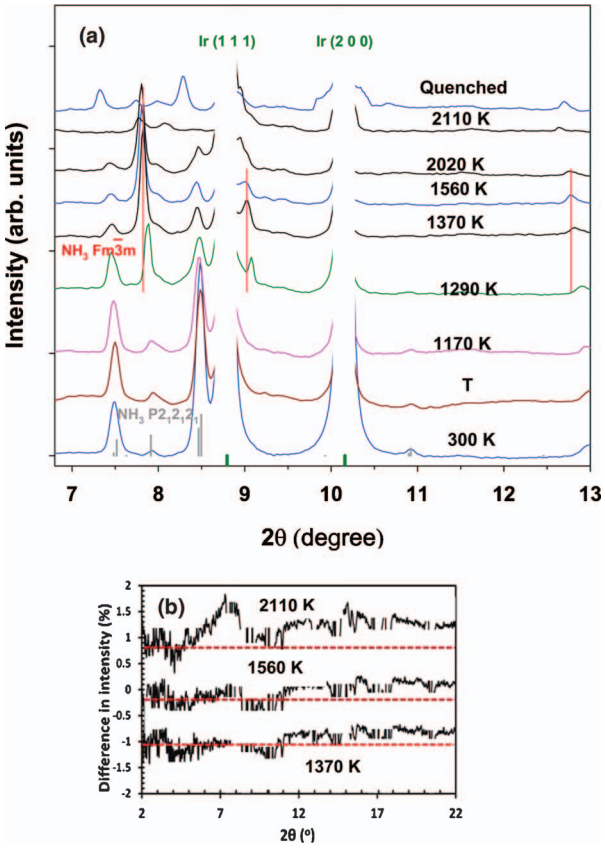

FIG. 5. Representative synchrotron x-ray diffraction ($\lambda = 0.3344$ Å) patterns, background-corrected, of NH_3 collected at 24 GPa as a function of temperature. Green and red tick marks indicate the allowed reflections for $Fm\bar{3}m$ structure with lattice parameter $a = 3.793$ Å (Ir) and $a = 4.244$ Å (NH_3-III), respectively, while gray tick marks indicate the allowed reflections for $P2_12_12_1$ structure (NH_3-IV). The strong peaks of Ir, indicated by green tick marks, are masked. Remnants of Bragg peaks of solid NH_3 remain even at the highest temperature because of large axial temperature gradients (see Sec. II). Panel (b) shows the appearance of a diffuse halo corresponding to fluid NH_3 above the melting temperature. The diffuse halo is very weak and cannot be seen in the scale of the main figure (a). Thus, we plotted the difference in intensity between the patterns measured at different temperatures and that measured at 300 K, to subtract the incoherent and background scattering;[16] at 2110 K, a diffuse scattering halo associated with liquid NH_3 is clearly seen. Narrow Bragg peaks corresponding to solid phases are omitted for clarity. Dashed red lines in (b) are the baselines shifted vertically for clarity.

well, but is somewhat higher than that obtained in the resistively heated DAC.[10] This difference emanates from the fact that our temperature measurements are based on spectroradiometry of the coupler, which is at higher temperatures than the bulk of the sample being probed.[32] Thus, the melting points obtained in this work should be considered an upper bound. On the other hand, the discrepancy in the IV(V)-III transformation line is too large to be accounted for by temperature gradients alone. We suggest that kinetics and, perhaps, sample confinement effects (e.g., Ref. 33) play an important role in this transition, which is further supported by a strong hysteresis or time dependence of transformation evidenced by observations of quenching of high-temperature NH_3-III to room temperature (Figs. 2(a) and 2(b)). The IV(V,VI)-III transition could not be detected above 50 GPa; this suggests the presence of a triple point near 60 GPa and 1500 K.

Our results show that the melting curve has a maximum at 37 GPa ± 6 GPa (2140 K ± 200 K), strongly deviating from the Simon-Glatzel law,[34] so we fitted the data using the Kechin[35] melt equation (Fig. 1). Our melting line disagrees with that predicted by Cavazzoni *et al.*[2] based on AIMD simulations. Indeed, our data suggest a negative slope of the melting line in the pressure range where Cavazzoni *et al.* predict it to be strongly positive. The Raman spectra of fluid (Fig. 2(d)) show a substantial N–H stretch peak broadening following the melting line flattening similar to that observed in water[36] and nitrogen,[17] where the effects of intermolecular atomic fluctuations were inferred based on such observations.

Laser heating of NH_3 above the melt line causes a very intense light emission (or flash) along the boundary approximately outlined in Fig. 1. This boundary was determined from the temperatures measured immediately before the "flash" appears. Once the sample is subjected to these conditions, the Raman spectra of the quenched products show a drastically increased amount of the H_2 and N_2 reaction products, while the signal from NH_3 is strongly reduced, indicating NH_3 depletion (Fig. 6). Moreover, the solid phases of NH_3 quenched to room temperature from these conditions are different from those that were initially heated (Figs. 2, 4, and 6). At $P \leq 15$ GPa, we observed that NH_3 quenches to NH_3-III (Figs. 2(a) and 2(b)), not the initial NH_3-IV; at higher pressure, phase V quenches to a modified phase, characterized by the presence of an additional N–H stretch mode (Fig. 4). Similarly, when heating NH_3-VI, we observed that the quenched phase was again different from the initial one; above 55 GPa (Fig. 6), we find a quench phase with a substantially modified Raman spectrum, featuring one extra N–H stretch band and a number of new strong bands in the phonon spectral range; the IR spectra of stretching and bending N–H modes did not show any substantial change (Fig. 6(d)). These changes characterize the formation of a new orientationally ordered molecular phase. The IR spectra of the quenched sample subjected to laser heating at 45–55 GPa (Fig. 6(b)) show an increased activity near and below 3000 cm^{-1}, the spectral range where N–H stretch modes of the NH_4^+ ion are expected.[6] The Raman spectra of this quenched sample show a substantial broadening of the N–H stretch and an almost total disappearance of the lattice modes.

V. DISCUSSION

The phase diagram of ammonia at HTHP conditions has much in common with the phase diagrams of other simple molecular materials, for example, water[36] and nitrogen,[17] including flattening of the melting line in the regime approaching molecular dissociation. This is related to a destabilization of covalent intramolecular bonds due to compression and the redistribution of electron density (e.g., Ref. 37). The fluid adapts to the new high-pressure bonding scheme more readily than solid phases under pressure, manifesting in the phase diagram topology as a maximum of the melting line (as the fluid is denser). Theoretical calculations[2,38] suggest that in H_2O and NH_3, the melting line should increase in slope abruptly because of the presence of a superionic phase. This has been confirmed experimentally for H_2O near 40 GPa,[36,39,40] while

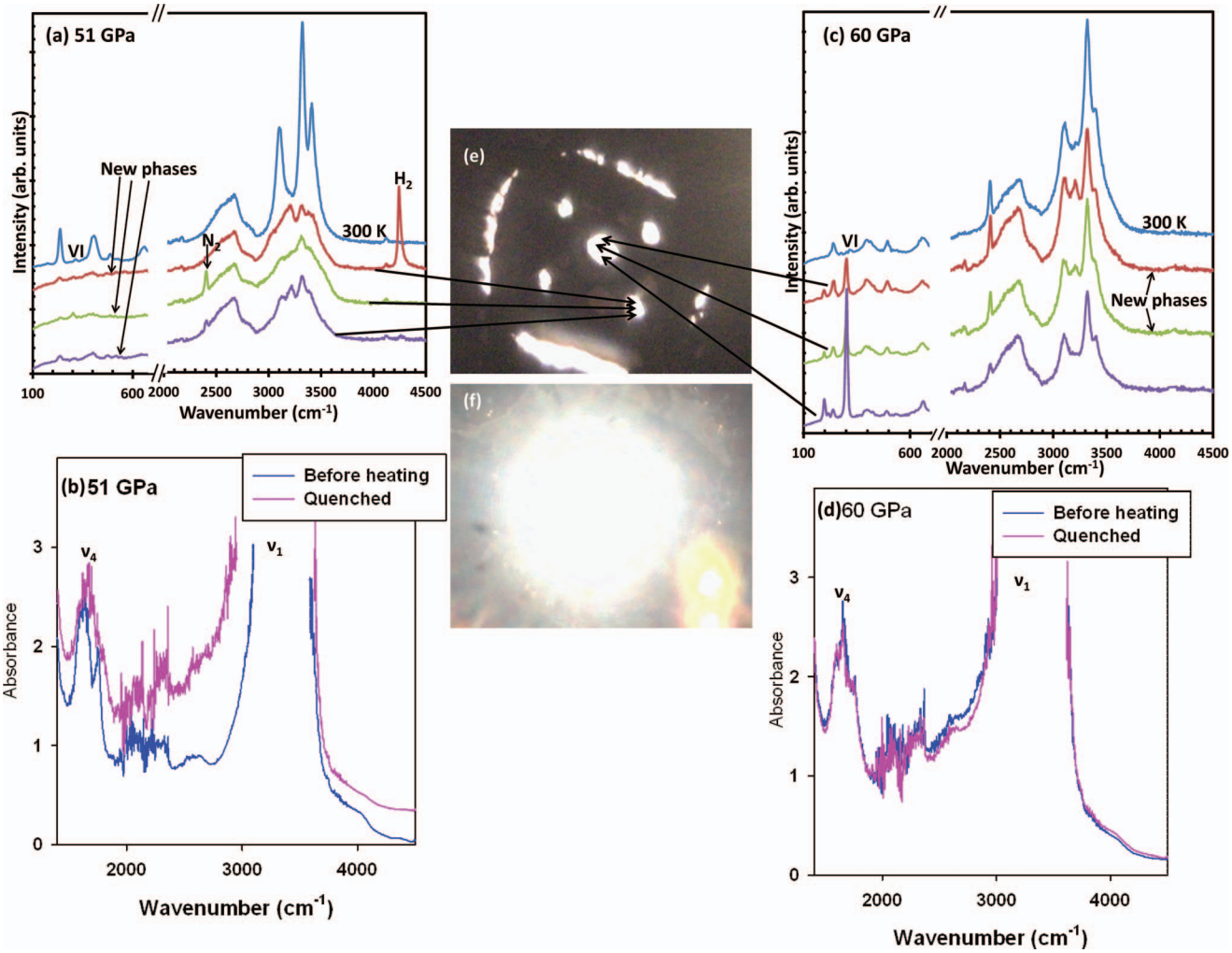

FIG. 6. (a)–(d) Raman and IR spectra of NH_3 (at 300 K and 51 and 60 GPa) before and after heating (quenched); Raman spectra are offset for clarity. Photos of sample holes in the Ir coupler (e) and the flash that appears at high laser power (f) are in the center. The lower right coupler hole was heated at 51 GPa until the appearance of flash, and quenched. The sample was then compressed to 60 GPa and the process was repeated for the central hole (the N_2 peak in the initial spectra is due to a previous heating cycle).

for NH_3, we did not find this increase in the slope up to 60 GPa, making the phase diagram of ammonia different from those of nitrogen and water.[17,36] We suggest that chemical reactivity is an additional factor which affects the phase stability of NH_3 at HTHP conditions. Alternatively, the theoretically proposed change in slope in ammonia may occur at higher pressures (>60 GPa), as the recent report of a superionic phase of ammonia ice, stable at pressures above 57 GPa and temperatures above 700 K,[41] would suggest.

Our study shows that molecular NH_3 is chemically unstable, with respect to dissociation into H_2 and N_2 at extreme conditions. At ambient conditions, NH_3 is thermodynamically stable with respect to dissociation as its bond energy is larger than for constituents (the standard energy change of formation[42] $\Delta_f G = -12.67$ kJ/mol). Application of pressure and temperature must shift this inequality to account for the observed dissociation if it is caused by thermodynamic (not kinetic) stimuli. To get a better insight on our experimental results, we have performed *ab initio* calculations to compare the Gibbs free energies of solid ammonia with a mixture of fluid H_2 and N_2 (in the 3:1 proportion) to 900 K. We find that, at 700 K, ammonia is thermodynamically unstable above 8.8 GPa (Fig. 7). The examination of temperature dependent Gibbs free energy reveals (Fig. 8) that this instability is driven by the entropy of mixing term of $0.5\,N_2 + 1.5\,H_2$, which dominates over the entropy term of NH_3 at high temperature. Our experiment (Figs. 1 and 2(a)) shows the temperature of onset of dissociation in a fair agreement with calculations. The line of intense chemical dissociation (Fig. 1), which we find to occur at higher temperatures, must be related to nonequilibrium processes since it results in irreversible transformations. They might be related to a resonant absorption of a heating laser light quanta.

Fluid-phase vibrational spectroscopy (Fig. 2(d)) and observations of chemical dissociation (Figs. 2–4 and 6) suggest that NH_3 fluid at high pressures is largely dissociated either dynamically (evidenced by the broadening of the N–H stretch band analogous to the N–N and O–H stretch modes in nitrogen and water in Refs. 17 and 36, respectively, suggesting the presence of intermolecular proton

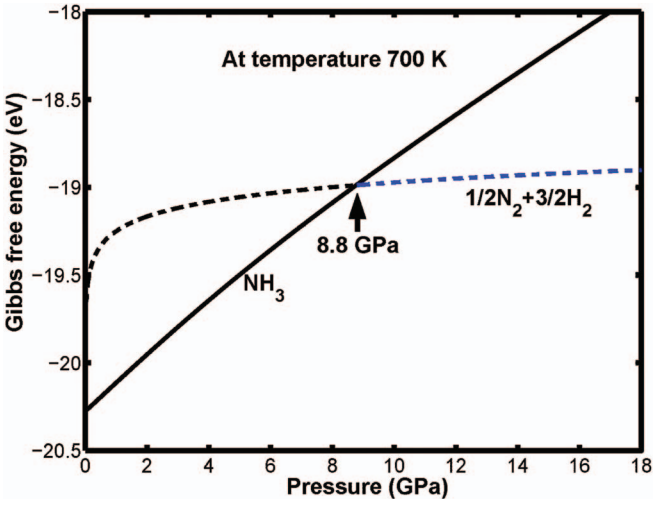

FIG. 7. Gibbs free energy of ammonia in comparison to that of $\frac{1}{2}N_2 + 3/2H_2$ mixture at 700 K (blue thick lines).

fluctuations), or chemically (evidenced by the formation of diatomic reaction products). However, in the case of ammonia, the chemical decomposition of NH_3 becomes energetically competitive at less extreme conditions compared to ionization effects. These chemical decomposition phenomena can compete with more familiar ionization[2,5,36,43] at planetary interior conditions. Since N_2 and H_2 are strongly bonded nonionic molecules, the bulk conductivity within ammonia-rich planets such as Uranus and Neptune may be lower than predicted for a system consisting of fully ionized NH_3, though the chemistry of NH_3 in a mixture (i.e., with H_2O and CH_4) could differ from that observed in the pure phase.[43] Molecular nitrogen present in deep planetary interiors could also be brought to the surface via convective processes and contribute to the observed abundances of nitrogen in the atmospheres of planets such as Neptune.[44,45]

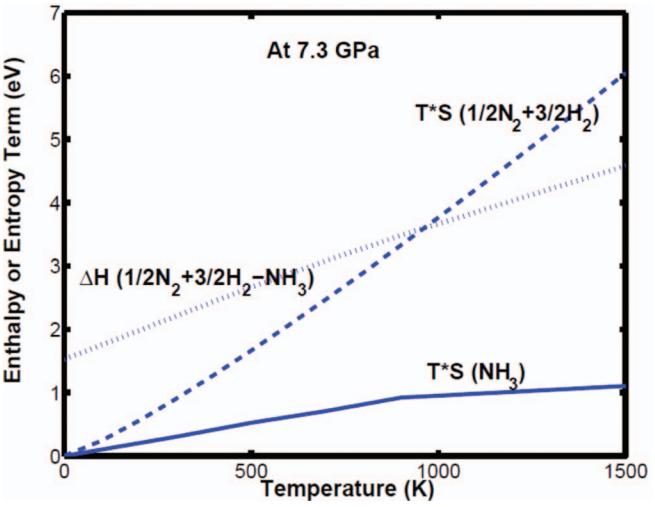

FIG. 8. Calculated enthalpy difference for $\frac{1}{2}N_2 + 3/2H_2 - NH_3$ and entropy of $\frac{1}{2}N_2 + 3/2H_2$ and of NH_3 at 7.3 GPa.

VI. CONCLUSION

Our experimental and theoretical results on ammonia at HTHP conditions show a turnover of the melting line above 37 GPa, which is followed by a continuous change in the bonding character of fluid manifested by a dramatic broadening of the N–H stretch band. We interpret these changes as due to an increase of intermolecular proton fluctuations. We also find, based on the Raman measurements and theoretical *ab initio* calculations, that solid ammonia becomes unstable with respect to dissociation to diatomic molecules. This chemical reactivity increases dramatically in the laser-heated fluid state in correspondence with phase changes in unreacted ammonia. We propose that chemical reactivity competes with ionization phenomena in NH_3 at extreme conditions. Our data suggest that the predicted superionic state (if any) can be realized above 60 GPa in agreement with recent observations in the resistively heated DAC.[41]

ACKNOWLEDGMENTS

We thank M. Somayazulu for extensive help with sample preparation and characterization; M. Mahmood, T. Strobel, M. Guthrie, and R. J. Hemley for comments on the manuscript; N. Subramanian for support with laser heating software at the Geophysical Laboratory; and V. Prakapenka for excellent support of laser heating experiments at GSECARS. This work was supported by the National Science Foundation Division of Earth Sciences, the U.S. Army Research Office, NASA Astrobiology Institute (NAI), Department of Energy (DOE)/National Nuclear Security Administration (Carnegie DOE Alliance Center), and Carnegie Institution of Washington. The x-ray diffraction measurements were performed at GSECARS (APS) supported by the DOE (Contract No. W-31-109-Eng-38). Use of the Advanced Photon Source was supported by the U.S. Department of Energy, Office of Science, Office of Basic Energy Sciences (Contract No. DE-AC02-06CH11357).

[1] W. B. Hubbard, Science **214**, 145 (1981).
[2] C. Cavazzoni, G. L. Chiarotti, S. Scandolo, E. Tosatti, M. Bernasconi, and M. Parrinello, Science **283**, 44 (1999).
[3] W. J. Nellis, D. C. Hamilton, N. C. Holmes, H. B. Radousky, F. H. Ree, A. C. Mitchell, and M. Nicol, Science **240**, 779 (1988).
[4] W. B. Hubbard, W. J. Nellis, A. C. Mitchell, N. C. Holmes, S. S. Limaye, and P. C. McCandless, Science **253**, 648 (1991).
[5] R. Chau, S. Hamel, and W. J. Nellis, Nat. Commun. **2**, 203 (2011).
[6] C. J. Pickard and R. J. Needs, Nature Mater.**7**, 775 (2008).
[7] R. L. Mills, D. H. Liebenberg, and P. Pruzan, J. Phys. Chem. **86**, 5219 (1982).
[8] R. B. Von Dreele and R. C. Hanson, Acta Crystallogr., Sect. C: Cryst. Struct. Commun.**40**, 1635 (1984).
[9] J. S. Loveday, R. J. Nelmes, W. G. Marshall, J. M. Besson, S. Klotz, and G. Hamel, Phys. Rev. Lett. **76**, 74 (1996).
[10] S. Ninet and F. Datchi, J. Chem. Phys. **128**, 154508 (2008).
[11] S. Ninet, F. Datchi, S. Klotz, G. Hamel, J. S. Loveday, and R. J. Nelmes, Phys. Rev. B **79**, 100101(R) (2009).
[12] M. Gauthier, P. Pruzan, J. C. Chervin, and J. M. Besson, Phys. Rev. B **37**, 2102 (1988).
[13] F. Datchi, S. Ninet, M. Gauthier, A. M. Saitta, B. Canny, and F. Decremps, Phys. Rev. B **73**, 174111 (2006).
[14] A. F. Goncharov, J. A. Montoya, N. Subramanian, V. V. Struzhkin, A. Kolesnikov, M. Somayazulu, and R. J. Hemley, J. Synchrotron Radiat. **16**, 769 (2009).

[15]V. B. Prakapenka, A. Kubo, A. Kuznetsov, A. Laskin, O. Shkurikhin, P. Dera, M. L. Rivers, and S. R. Sutton, High Press. Res. **28**, 225 (2008).
[16]A. F. Goncharov, N. Subramanian, T. R. Ravindran, M. Somayazulu, V. B. Prakapenka, and R. J. Hemley, J. Chem. Phys. **135**, 084512 (2011).
[17]A. F. Goncharov, J. C. Crowhurst, V. V. Struzhkin, and R. J. Hemley, Phys. Rev. Lett. **101**, 095502 (2008).
[18]W. Kohn and L. J. Sham, Phys. Rev. B **140**, A1133 (1965).
[19]P. Hohenberg and W. Kohn, Phys. Rev. B **136**, B864 (1964).
[20]D. M. Ceperley and B. J. Alder, Phys. Rev. Lett. **45**, 566 (1980).
[21]G. Kresse and J. Furthmüller, Comp. Mat. Sci. **6**, 15 (1996).
[22]G. Kresse and J. Furthmüller, Phys. Rev. B **54**, 11169 (1996).
[23]P. E. Blöchl, Phys. Rev. B **50**, 17953 (1994).
[24]G. Kresse and D. Joubert, Phys. Rev. B **59**, 1758 (1999).
[25]H. J. Monkhorst and J. D. Pack, Phys. Rev. B **13**, 5188 (1976).
[26]K. Parlinski, Z. Q. Li, and Y. Kawazoe, Phys. Rev. Lett. **78**, 4063 (1997).
[27]K. Parlinski, Software PHONON, Institute of Nuclear Physics, Crakow, 2005.
[28]A. A. Maradudin, E. W. Montroll, G. H. Weiss, and I. P. Ipatova, *Theory of Lattice Dynamics in the Harmonic Approximation in Solid State, Physics Supplement* (Academic, New York, 1971), Vol. 3.
[29]H. Olijnyk and A. P. Jephcoat, Phys. Rev. Lett. **83**, 332 (1999).
[30]H.-K. Mao and R. J. Hemley, Rev. Mod. Phys. **66**, 671 (1994).
[31]H. Schneider, W. Häfner, A. Wokaun, and H. Olijnyk, J. Chem. Phys. **96**, 8046–8053 (1992).
[32]E. Gregoryanz and A. F. Goncharov, Phys. Rev. Lett. **102**, 049601 (2009).
[33]M. R. Silvestri and J. Schroeder, J. Phys.: Condens. Matter **7**, 8519 (1995).
[34]E. Simon and G. Glatzel, Z. Anorg. Allg. Chem. **178**, 309 (1929).
[35]V. V. Kechin, Phys. Rev. B **65**, 052102 (2001).
[36]A. F. Goncharov, N. Goldman, L. E. Fried, J. C. Crowhurst, I.-F. W. Kuo, C. J. Mundy, and J. M. Zaug, Phys. Rev. Lett. **94**, 125508 (2005).
[37]R. J. Hemley, Annu. Rev. Phys. Chem. **51**, 763 (2000).
[38]E. Schwegler, M. Sharma, F. Gygi, and G. Galli, Proc. Natl. Acad. Sci. U.S.A. **105**, 14779 (2008).
[39]J.-F. Lin, E. Gregoryanz, V. V. Struzhkin, M. Somayazulu, H. K. Mao, and R. J. Hemley, Geophys. Res. Lett. **32**, L11306, doi:10.1029/2005GL022499 (2005).
[40]B. Schwager, L. Chudinovskikh, A. Gavriliuk, and R. Boehler, J. Phys.: Condens. Matter **16**, S1177 (2004).
[41]S. Ninet, F. Datchi, and A. M. Saitta, Phys. Rev. Lett. **108**, 165702 (2012)
[42]*CRC Handbook of Chemistry and Physics*, 42nd ed. (CRC, 1960), pp. 1882–1915.
[43]M. Lee and S. Scandolo, Nat. Commun. **2**, 185 (2011).
[44]A. Marten, D. Gautier, T. Owen, D. B. Sanders, H. E. Matthews, and S. K. Atreya, Astrophys. J. **406**, 285 (1993).
[45]E. Lellouch, P. N. Romani, and J. Rosenqvist, Icarus **108**, 112 (1994).